T. Teumer, C. Capitain, J. Ross-Jones, N. Tippkötter, M. Rädle and F.-J. Methner

In-line Haze Monitoring Using a Spectrally Resolved Back Scattering Sensor

In the present work an optical sensor in combination with a spectrally resolved detection device for in-line particle-size-monitoring for quality control in beer production is presented. The principle relies on the size and wavelength dependent backscatter of growing particles in fluids. Measured interference structures of backscattered light are compared with calculated theoretical values, based on Mie-Theory, and fitted with a linear least square method to obtain particle size distributions. For this purpose, a broadband light source in combination with a process-CCD-spectrometer (charge – coupled device spectrometer) and process adapted fiber optics are used. The goal is the development of an easy and flexible measurement device for in-line-monitoring of particle size. The presented device can be directly installed in product fill tubes or vessels, follows CIP- (cleaning in place) and removes the need of sample taking. A proof of concept and preliminary results, measuring protein precipitation, are presented.

Descriptors: fiber optical sensor, beer quality monitoring, Mie Theory, particle size measurement, process control, haze

1 Introduction

The monitoring of coagulation, precipitation and crystallization plays an important role in quality control and reliability for food production and storage processes. The turbidity and haze formation of beer affects quality and storage stability of beer. Thus, the in-line monitoring of contaminants and slow growing particles, simplifies stability testing procedures for the detection of haze formation and probably ensures a more precise prediction of expected expiry dates.

Literature differentiates between native particles such as proteins, polyphenols and glucans which originate from the raw ingredients for brewing as shown by *Rehmanji* et al. [1], inorganic particles, which originate from filter aids or inadequacies in the equipment cleaning processes and lastly, foreign contaminants such as bacteria, which enter the beer unintentionally as described by *Juvonen* et al. [2]. Furthermore, haze formation can develop even in filtered beer, after prolonged storage. This is intensified by temperature fluctuations as shown by *Siebert* et al. [3] and in the MEBAK [4].

https://doi.org/10.23763/BrSc18-06teumer

Authors

Tobias Teumer, Jesse Ross-Jones, Matthias Rädle, CeMOS – Center of mass spectrometry and optical spectroscopy, Mannheim University of Applied Sciences, Mannheim, Germany; Charlotte Capitain, Institute of Bioprocess Engineering, University of Kaiserslautern, Kaiserslautern, Germany; Nils Tippkötter, Institute of Bioprocess engineering, University of Applied Sciences Aachen, Jülich, Germany; Frank-Jürgen Methner, Chair of Brewing Science, Institute of Food Technology and Food Chemistry, Technische Universität Berlin, Berlin, Germany; corresponding author: t.teumer@hs-mannheim.de

For a reduction or removal of the precipitation tendencies and to avoid undesired haze formation, additional clarifying agents are used. The varieties of particles present need to be differentiated. An early stage detection of such contaminants will help to optimize the stability of beer and avoid long-term stability testing.

Commonly used particle sizing methods in liquids include optical microscopy (OM). This method allows precise size characterization, but has limited throughput shown by *Satinover* et al. [5]. Moreover, optical microscopy involves the use of expensive stationary equipment and is limited to a detection range between 2 % and to 40 % of the orifice diameter of the measurement tube. Newer attempts at particle size characterization use forward scattering (laser diffraction, LD). However, this method can only be employed when higher concentrations of the particles of interest, are present. A measured mean size variability of 7.1 % was reported, when using LD as compared to OM, which obtained a mean diameter sizing variability of only 1.1 % shown by Satinover et al. [5].

The lack of accurate information about imaginary and real components of the refractive indices, as well as non-spherical and non-homogeneous particles, is a well-known challenge for methods involving light scattering. However, in a well-defined environment, like beer, where all particles can be characterized, this can be turned into an advantage. It is proposed that through inverse calculation of light scattering intensities together with possible refractive indices, conclusions about the particle nature can be made. In-line monitoring of particles using spectrally resolved scattering sensors could be an inexpensive and fast in-line-method for the measurement of both, particle concentration and particle size. Additionally, this method allows determining the size of particles as small as 250 nm, as well as the detection gradually changing particle size distributions shown by *Gulari* et al. [6].

The state of the art in quality management in the brewery industry is product control according to MEBAK regulations [4]. These

regulations include a wide list of trusted analytical methods and equipment which can be used in the brewing process. Since optical process control and quality management tools are already approved for turbidity measurements during the lautering process shown in MEBAK [4], the equipment used in this work already conforms to the MEBAK-regulations.

2 Theory

2.1 Backscattering Principle

Laser light scattering occurs when an incident waveform interacts with a particle. The backscattering component of this interaction is used as measuring principle in this work. In addition to scattering laser light can also be absorbed by the particle shown by *Mishchenko* et al. [7] and *Horvarth* et al. [8]. When light is absorbed the irradiation energy is converted to heat shown by *Roy* et al. [9]. In contrast, during elastic scattering the incoming light ray changes direction without changing energy level. Scattering can also be categorized into refraction, reflection or diffraction from the surface of a particle. When the resulting light wave acquires only a small deflection angel, the scattering process is considered forward scattering. When the scattering angel, however, is between 90° and 180° to its incident direction, this is considered back scattering.

The intensity of scattering depends on the wavelength of the scattered light as well as the particle size. Furthermore, scattering patterns depend on the scattering angle and the density of the particle suspension. In this work, these features are used for particle size analysis. First, the characteristic scattering pattern for different particle sizes are generated using the Mie theory shown by Mishchenko et al. [7] and by Horvarth et al. [8] and the software MiePlot programmed by *Laven* et al [10]. The software calculates scattering intensities according to Mie theory for spherical particles, which applies when the particle radius is approximately as large as the wavelength of the incoming light as shown by *Schmidt* et al. [11]. Using scattering patterns for the determination of the size distributions is a common method in scientific and industrial processes, it is currently state of the art as well as a cost-effective alternative to microscopic analysis. Following, a few examples for particle size determination are given. Gulari et al. [6] determined particle size distribution of latex suspensions by measuring the turbidity of the suspension. In the work done by *Mundy* et al. [12] a comparison of turbidity measurement equipment from diverse manufacturer are presented, therein, defined calibration particles were measured. These standards were monodisperse suspension systems with particles ranging in size between 0.5 µm and 2 µm. The measurements took place between 90° and 13°. *Polke* et al. [13] describe in detail several measuring systems to determine particle size. With the help of photon counting systems, the size distribution was obtained. For this purpose, scattered light impulses were counted, which occur when particles intersect with a parallel light beam during their passage through a special measuring chamber. The shadow of the particle is measured with a charge – coupled device chip, which equates to the particle size. Simultaneous recordings of back scatter patterns of different aerosol particles, which are measured through laser trapping, were shown by *Fu* et al. [14]. *Dautzenberg* et al. [15] traced precipitation kinetics of a low concentrated polymer solution with the help of a scattered light photometer at an angel of 45°.

Currently, the presence of beer haze is detected with a standardized measuring principle available in MEBAK using scattered light at an angle of 90° using only one wavelength shown in MEBAK [5], and in Polke et al. [13]. However, only the level of beer haze is measured by this method. In contrast, the present work measures in the first place light scattered at 180° over a range of wavelengths and secondly, is able to indicate the mean particle size.

2.2 Mie Theory

Mie theory is a mathematical model that describes the scattering of light caused by particles when the particle size and wavelength of the light have similar dimensions. In this work, Mie theory is applied for particle size analysis of microscopic particles shown by *Kraemer* et al. [16]

Mie-scattering or Lorenz-Mie-scattering is based on a mathematic description of electromagnetic scattering of a plane wave when encountering a sphere. Whereby, the incident plane wave and the scattered electro-magnetic field are described as a series of spherical wave functions. The scattered waves are divided into three categories: the incoming wave with field $(\mathrm{E1}, \mathrm{H1})$, the electromagnetic wave inside the particle with field $(\mathrm{E2}, \mathrm{H2})$ and scattered wave with the field $(\mathrm{E3}, \mathrm{H3})$. The incoming wave is defined in polar coordinates. For the waves inside the sphere and the scattered waves, the electro-magnetic fields are expressed with the Hertz Debey potential π in Equation 1. This potential is formed through a sequential approach based on Legendre polynomial $P_n^{(m)}(cos(\theta))$ and the Ricatti-Bessel functions Ψ_n and by $\mathrm{X_n}$ Ray et al. [17]:

$$r\pi = \sum_{n=0}^{\infty} \sum_{m=-n}^{n} \pi_n^{(m)} \qquad \textbf{Eq. 1}$$

$$\pi_n^{(m)} = \{c_n \Psi_n(kr) + d_n \mathrm{X}_n(kr)\} \cdot \left\{P_n^{(m)} \cdot (\cos\vartheta)\right\} \cdot \{a_m \cdot \cos(m\varphi) + b_m \cdot \sin(m\varphi)\}$$

where a_m, b_m, c_n, and d_n are scattering coefficients. The Ricatti-Bessel-functions are formed from the Bessel and Neumann functions $I_{(\mathrm{n}+1/2)}$ und $\mathrm{N}_{(\mathrm{n}+1/2)}$ respectively shown in Equation 2.

$$\Psi_n(kr) = (\pi kr/2)^{1/2} \cdot \mathrm{I}_{n+1/2}(kr) \qquad \textbf{Eq. 2}$$

$$\mathrm{X}_n(kr) = (\pi kr/2)^{1/2} \cdot \mathrm{N}_{n+1/2}(kr)$$

The functions $\mathrm{X(kr)}$ show a singularity at point $\mathrm{kr} = 0$. For the display only the $\Psi(\mathrm{kr})$ values are used for the waves inside the sphere. In a special linear combination where $\mathrm{cn} = 1$ and $\mathrm{dn} = \mathrm{i}$ the Hankel function H, see Equation 3, approaches infinity.

$$\zeta_n(kr) = \mathrm{X_n(kr)} + \mathrm{i}\Psi_\mathrm{n}(\mathrm{kr}) = (\pi \mathrm{kr}/2)^{1/2} \mathrm{H}^2_{\mathrm{n}+1/2}(\mathrm{kr}) \qquad \textbf{Eq. 3}$$

Therefore, this description can be used to describe the scattering wave. To determine the scattering coefficients a_m, b_m, c_n, and d_n and from the boundary conditions, the potential functions (S) from the incoming wave, the wave inside the sphere and the scattering

wave are needed. With the boundary conditions, a series of linear equations are formed from which the coefficients can be determined. They depend on size parameter (X) and the relative refractive index (m). Both parameters can be derived from the sphere radius (r), light wavelength (λ), refractive index of the sphere (n) and refractive index (n_0) of the surrounding medium by Ray et al. [17].

$$X = \frac{2\pi r}{\lambda} \qquad \text{Eq. 4}$$

$$m = \frac{n}{n_0} \qquad \text{Eq. 5}$$

Once the size parameter (X), Equation 4, and the relative refractive index (m), Equation 5, are obtained, the scattered light encountering a sphere can be described.

Both of these parameters can be determined when the scattered light intensity is measured, as a function of the wavelength, and then compared to theoretical values. Moreover, there is a distinction between near field and far field stray waves. The radial components of the stray field decrease quadratically as a function of the radius $(\alpha\, r^{-2})$, and the orthogonal component decreases linearly as a function of the radius $(\alpha\, r^{-1})$. Thus, at a distance, the wave is recognized as being purely transversal. In addition, there are significant changes in the intensity as a function of the wavelength when small changes in the particle size or in the refractive index of the particle or the surrounding medium occur. The number of maxima in the backscattering spectrum increases proportionally with the particle radius. Therefore, by measuring the changes in light intensity as a function of the wavelength, then comparing the measurement to theoretical Mie scattering, inferences about the particle size can be made. The backscattered intensity distribution can be detected and inversely calculated to obtain the properties for an equivalent spherical particle system through the Mie equations.

3 Material and methods

3.1 Particles and proteins

Spherical Micromer® polystyrene particles (PS) were obtained from Micromod Partikeltechnologie GmbH, Germany, with particle diameters of 0.5 µm (PDI < 0.2, PDI = polydispersity index und CV = coefficient of variance) and 1 µm (PDI < 0.2). For backscattering measurements, the particle solution was dissolved in purified water until a transmission ratio of 0.9 was reached compared to the purified water without particle. To remove the influence of the water medium and obtain the back scattering spectra for the polystyrene particles reference measurements were taken using purified water.

The wheat protein fraction glutenin, which is further referred to as 'protein', was extracted from gluten (Sigma Aldrich, ≥ 80 % protein). The protein was homogeneously dissolved in purified water (2–8 °C). The solution was adjusted to pH 9 where a first precipitation occurred and filtered through a prepleated filter (Whatman 597 1/2). The clear filtrate (at pH 12) was used for reference measurements to remove the influence of the water and obtain the back scattering spectra for the protein. The pH was regulated using a 0.1 M NaOH solution (Merck Millipore) and 0.1 M HCl solution (Merck Millipore) between pH 5 to pH 6 where the back scattering measurements took place. Subsequently, 1 mL of the homogenized suspension was extracted in order to determine the size of proteins using optical microscopy with an Olympias CX31, shown in figure 1.

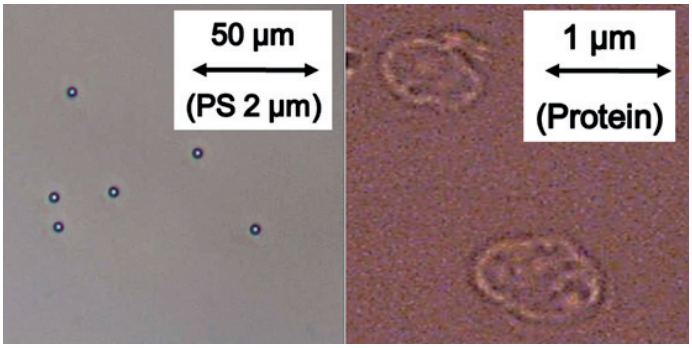

Fig. 1 Polystyrene particles (left) and protein particle (right) measured with optical microscope

3.2 Experimental set-up and measuring procedure

The fiber optical test setup used, is visualized in figure 2. The setup consists of a light source (halogen bulb lamp, CL H 600, from the company Zeiss), a back scattering probe (7 fiber reflection probe 400 µm, UV/VIS, 6 light emitting fibers and 1 detection fiber, from the company Oceanoptics) plus a CCD-spectrometer (MCS 6210 VIS II, from the company Zeiss). For each measurement, the probe is placed in a static homogenized suspension. The probe is adjusted in a beaker such that the probe tip is at an angel of 25° to 30° to the beaker wall. This is necessary to avoid the possibility of measuring the reflection from the bottom glass surface. The spectra are recorded using the software Aspekt Plus. For data evaluation, the wavelengths section between 500 nm and 800 nm is used. Under 500 nm Mie effects can be masked due to fluorescence phenomena. Mie scattering effects can be detected using wavelengths up to 800 nm. Several full spectrum measurements are taken per second.

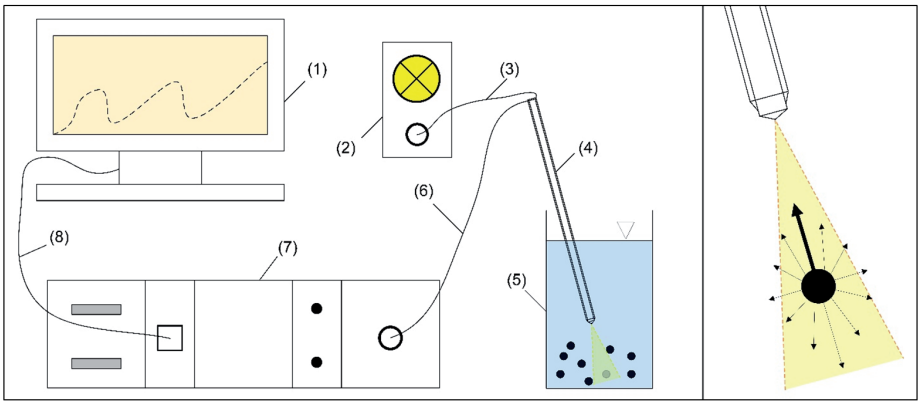

Fig. 2 Test set up for backscatter measurements

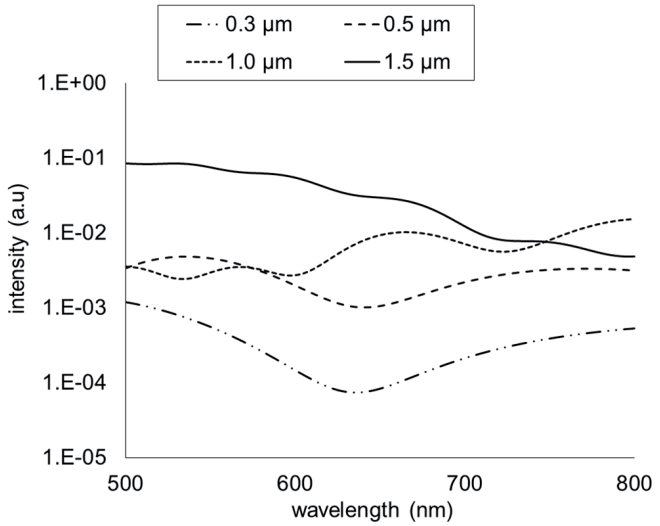

Fig. 3 Calculated back scattering intensity versus wavelength using MiePlot

3.3 Computational analysis of back scatting profiles using linear least squares

Linear least squares is mathematical or statistical approach for fitting a model to data in cases where the value provided by the model is expressed linearly in terms of the unknown parameters of the model.

In this work, Mie theory simulations are compared with real measurements. A fitting algorithm and an appropriate program for describing the mean or median particle size was developed. A database based on Mie theory was generated simulating wavelength dependent backscatter patterns at 180 degrees for particles ranging from 0.3 µm to 1.5 µm in diameter, over a step size of 10 nm. The simulation calculates the backscattering intensity over a range of wavelengths starting from 500 nm to 800 nm. The simulation requires an expected refractive index, in this case, refractive indices for polystyrene and protein are used. Figure 3 shows the simulated intensity of four different particle sizes (0.3 µm, 0.5 µm, 1.0 µm and 1.5 µm) for wavelengths between 500 and 800 nm.

The following terms are used to describe the measurement, simulation and reconstruction curves present in the graphs presented in this work:

- Measured/Measurement: curves measured with the experimental setup described in this work to measure the back scattering intensity.
- Simulated: curves that were simulated using Mie theory.
- Reconstruction/Fitted: curves which use the subsequently described linear least square algorithm to reconstruct the measured curves using a combination of Mie back scattering curves.

The pseudo code below outlines the steps used to preprocess and arrange the measurement data into a formal solvable using a least squares solver.

- [startWavelength = 500
- endWavelength = 800
- proteinBackscatter = readSignal('backscatterProteinSignal.txt')
- databaseProtein = readDatabase('proteinBackscatterSim.txt')
- proteinBackscatter = crop(proteinBackscatter, startWavelength, endWavelength)
- databaseProtein = crop(databaseProtein, startWavelength, endWavelength)
- proteinBackscatter = setMin2Zero(proteinBackscatter) #Shift signal all values positive
- C = databaseProtein
- d = proteinBackscatter
- lb = zeros(length(C))]

This data can then be used with a least squares solver which is able to find solutions of the form Equation 6.

$$\min_x \frac{1}{2}||C \cdot x - d\,||_2^2$$
$$subject\ to{:}\ lb \leq x \qquad \textbf{Eq. 6}$$
$$y = C{*}x;$$

The previously mentioned code is described as follows. First, the measurement and simulated data is imported. Following, the data is cropped to the wavelengths of interest. Thereafter, to ensure that the simulated backscattering curves only interact constructively, the curves are each shifted such that the minimum of each signal lies at zero. The resulting matrix is defined to be C. Furthermore, a lower bound is set, such that the least squares solver only provides solutions where each component contributing to the particle size distribution (x) is greater than zero. Lastly, by setting d to be the measured protein backscattering data, and passing them to a least squares solver such as lsqlin in Matlab, a solution for x can be computed. The solver finds the minimum feasible solution to x in the Equation 7

$$\frac{1}{2}||C \cdot x - d\,||_2^2 \qquad \textbf{Eq. 7}$$

which is the squared 2-norm. The solver is able to apply several constraints the inequality and equality constraints were not used,

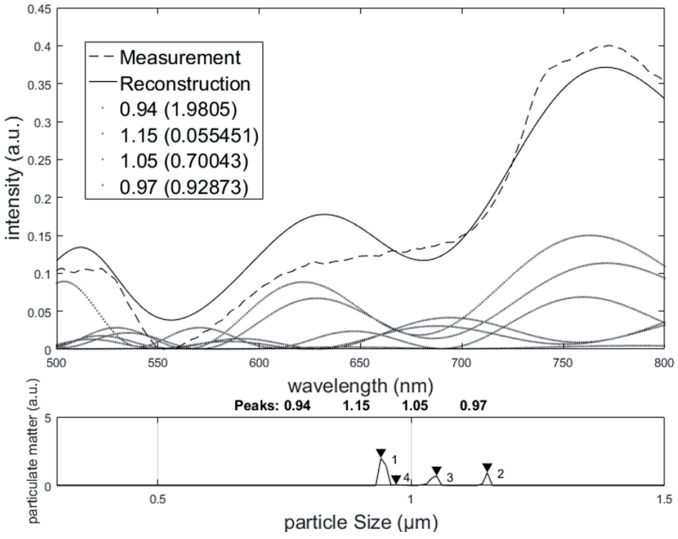

Fig. 4 Sample reconstruction of aqueous protein back scattering measurementusing linear least squares based on Mie scattering

only the lower bound constraints were used to avoid negative values.

To obtain the reconstructed backscatter intensity, the least squares solution (x) can be multiplied with the simulation database (C). The resulting vector (y) is a reconstruction of the original backscattering signal measured (d) measured.

An example reconstruction of the aqueous protein solution can be seen in figure 4. In addition to the measurement curve and the linear least squares reconstruction. The individual curves which linearly contribute to the reconstruction are visualized. Moreover, a histogram outlining which particles are present in the reconstruction can also be seen.

4 Results and Discussion

Measurements of monoidal and bimodal particle systems with sizes of 0.5 µm and 1.0 µm as shown in figure 5, figure 6 and figure 7 were used to verify the method, ensuring that the fitting algorithm was able to properly characterize the particle size. The measurement signals were reconstructed using linear least squares to find the best fit. The result is a linear combination of scattering curves from the database of simulated backscatter, over various particle sizes, reconstructing the measured backscatter.

Figure 5 and figure 6 show the curves of backscattering intensity for the monomodal systems, while figure 7 shows the corresponding results using a mixture of 0.5 µm and 1.0 µm diameter particles. Based on the fit, a particle size cumulative distribution function (CDF) is generated in which the balance point (the median particle size) of the calculated particle size can be determined, shown in figure 8 (see page 54). The gradient of the curves provides information of the particle size distribution for the monodisperse PS particles.

The CDF for the 0.5 µm particles shows a balance point at 0.47 µm and for the 1.0 µm particles, two balance points near 1 µm can be seen. For the bimodal particle system, a first balance point at 0.47 µm and a second at 1.1 µm was detected. This result was used to validate the method to determine the mean particle size if a system. After successful implementation of backscattering for mono and bimodal particle sizes, the technique was applied to measure protein particles.

Measurements of backscatter signals for aqueous protein solutions were reconstructed with the algorithm described previously. Figure 9 (see page 54) shows the measured backscattering curves, as well as the corresponding reconstruction for two proteins with different size distributions.

The particle size distributions of the proteins were additionally measured with a microscope offline and are shown in figure 10 (see page 54) together with the reconstructed CDFs using the inline spectral measurements. The deviation between the two curves is for the most part due to Mie theory using ideal spheres while proteins are not perfect spheres. The gradient of the curves provides information regarding the particle size distribution of the protein particles. Using this proof of principle, it is shown that

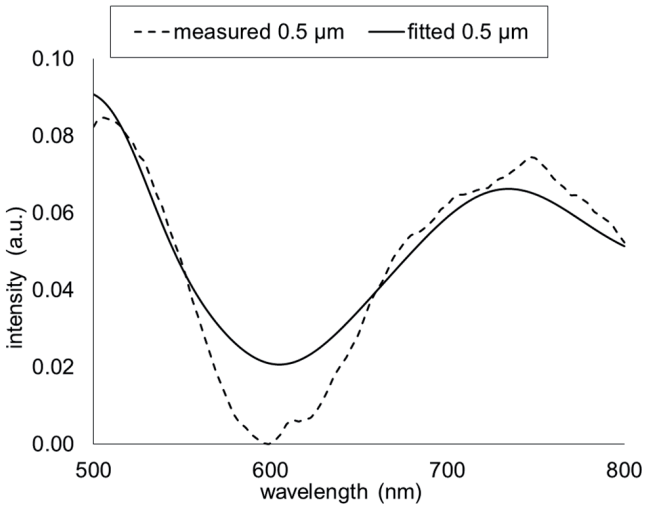

Fig. 5 Measured back scattering from polystyrene particles with 0.5 µm diameter together with least squares reconstruction based on Mie scattering

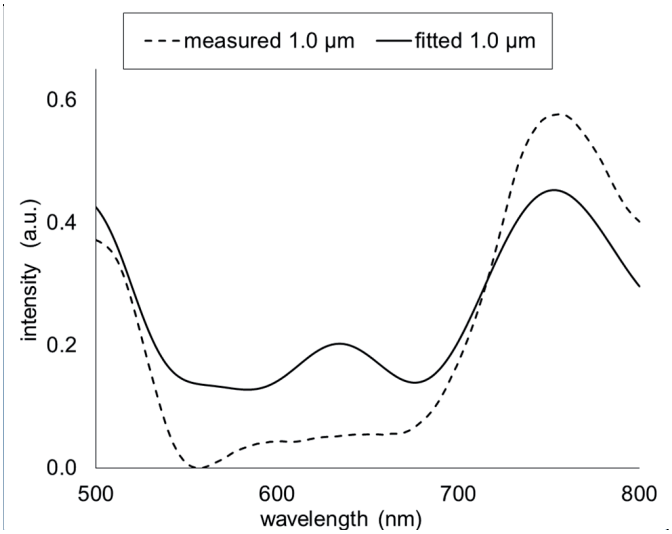

Fig. 6 Measured back scattering from polystyrene particles with 1.0 µm diameter together with least squares reconstruction based on Mie scattering

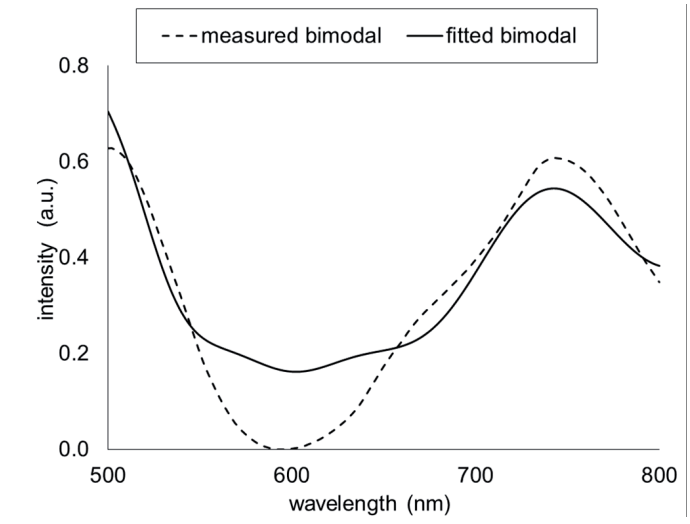

Fig. 7 Measured back scattering from polystyrene particle system with 0.5 µm and 1.0 µm diameter together with least squares reconstruction based on Mie scattering

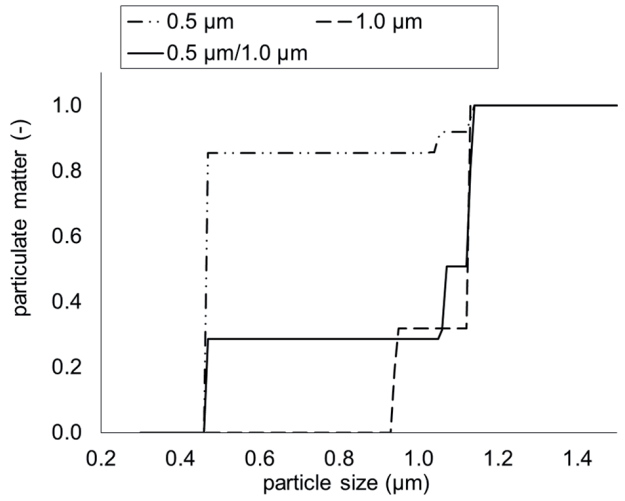

Fig. 8 Cumulative distribution function for the back scattering measurements of polystyrene particle systems

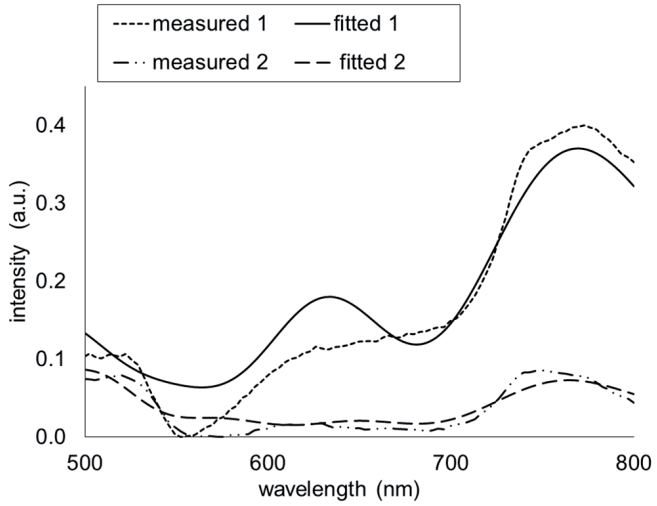

Fig. 9 Back scattering measured protein particle curves together with their respective least squares reconstruction based on Mie scattering

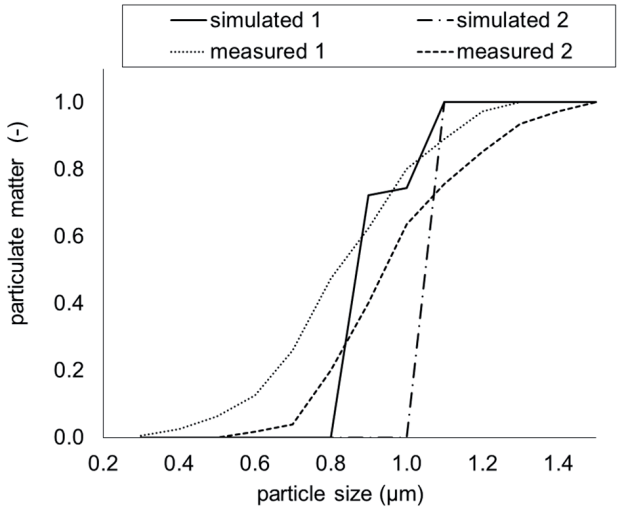

Fig. 10 Cumulative distribution functions for two different protein particle systems, comparing the reconstructed curves with those measured via microscopy

particle systems, such as proteins in beer haze, can be measured inline, with a single back scattering probe.

5 Conclusions

In this work, a linear least square (LLS) algorithm was used to fit scattering profiles of various particle sizes to those simulated with Mie theory, for the purpose of developing an in-line back scattering measurement system for particle size analysis in fluids. The detection frequency is high and allows several full spectrum measurements per second. This makes continuous monitoring of particle size, as well as local and temporal concentration possible. When applied to beer haze monitoring, the recognition of the species of the particles, which in beer are often proteins or oxalates, is possible. Early detection allows the brewer to quickly react and enact countermeasures against unwanted quality problems. The limitation of this measuring setup, for measuring particle size, is the physics behind the Mie theory in combination with the test setup in use. Only particles between 200 nm and 2000 nm can be currently measured. To detect the presence of particles smaller than 200 nm, the system would require additional capability of measuring Rayleigh scattering. The photosensitive detector would also require increased dynamic range and sensitivity due to the smaller particle sizes. To detect the presence of particles larger than 2000 nm, yeast cells could be used to calibrate the test setup and measure the Mie scattering for this particle size range. Furthermore, the CCD sensor would be replaced from a silicon based to an Indium/Gallium/Arsenid based one. The limiting factor would then be light transmittance through the optical fibers. The wavelength for the LLS algorithm would have to be set up with new parameters.

So far, the described system only allows the detection of the median particle size. In an extension to this work, the least squares solver could be extended to incorporate integer constraints. This enables additional system tuning. A constraint could be added, requiring the solution to be a special ordered set, meaning the curves must be closely clustered around one another to obtain a size distribution for monomodal particle systems or alternatively constraining the system to have a maximum of two solutions for measuring bimodal systems. Similarly, by modifying the constraints, multimodal systems can be described.

However, the median particle size distribution in combination with the particle concentration provides sufficient information for fast monitoring of changes in the overall quality. The small scale and simple design of the probe head allows for easy integration in various process environments, for example, in a continuous flow of wort after passing the lautering stage. Moreover, high pressures, high temperatures up to 180 °C or other conditions of CIP procedures do not interfere with the functionality of the probe head. The coupling of the sensor head to the electronic assembly using glass fibers keeps the dry and wet sections of the apparatus separate and allows for simple integration in rough production environments. The high throughput, cost effectiveness and ease of use of the system addresses the high demand of industrial systems. Now it is possible to react to fast changes in beer production systems. The described setup should now be put to the test in realtime brewery processes. Initially, the measurement could help measure wort quality during

the lautering stage. Later, it could be used as a process tool for intermediate beer quality control during the different filtering stages throughout the beer production process to test the beer quality. Finally, a measurement station at the end of the production line could be used to generate a stability forecast for the beer.

Acknowledgements

This work was funded by the German Federation of Industrial Research Associations (AiF Project GmbH).

6 Literature

1. Rehmanji, M.; Gopal, C. and Mola, A.: Beer Stabilization Technology – Clearly a Matter of Choice, Technical Quarterly, **42** (2004), no. 4, pp. 332-338.
2. Juvonen, R. and Haikara, A.: Amplification Facilitators and Pre-Processing Methods for PCR Detection of Strictly Anaerobic Beer-Spoilage Bacteria of the Class Clostridia in Brewery Samples, Journal of the Institute of Brewing, **115** (2009), no. 3, pp. 167-176.
3. Siebert, K. J.: Advances in Food and Nutrition Research, Chapter 2 Haze in Beverages, **57** (2009), Elsevier, pp. 53-86.
4. Miedaner, H. and Mitteleuropäische Brautechnische Analysenkommission: Eds. Brautechnische Analysenmethoden: Methodensammlung der Mitteleuropäischen Brautechnischen Analysenkommission (MEBAK). Bd. 2, 4. Aufl., neubearbeitet und ergänzt. (2002), Freising-Weihenstephan: Selbstverl. der MEBAK, pp. 4-7, pp. 92-95.
5. Satinover, S. J.; Dove, J. D. and Borden, M. A.: Single-Particle Optical Sizing of Microbubbles, Ultrasound in Medicine & Biology, **40** (2014), no. 1, pp. 138-147.
6. Gulari, E.; Bazzi, G.; Gulari, E. and Annapragada, A.: Latex Particle Size Distributions from Multiwavelength Turbidity Spectra, Particle & Particle Systems Characterization, **4** (1987), no. 1-4, pp. 96-100.
7. Mishchenko, M. I.: Gustav Mie and the fundamental concept of electromagnetic scattering by particles: A perspective, Journal of Quantitative Spectroscopy and Radiative Transfer, **110** (2009), no. 14-16, pp. 1210-1222.
8. Horvath, H.: Gustav Mie and the scattering and absorption of light by particles: Historic developments and basics, Journal of Quantitative Spectroscopy and Radiative Transfer., **110** (2009), no. 11, pp. 787-799.
9. Roy, D. and Fendler, J.: Reflection and Absorption Techniques for Optical Characterization of Chemically Assembled Nanomaterials, Advanced Materials, **16** (2004), no. 6, pp. 479-508.
10. Laven, P.: MiePlot website, MiePlot v4511, http://www.philiplaven.com/mieplot.htm, Version: March 2015
11. Schmidt, W.: Optische Spektroskopie: eine Einführung, 2. Aufl. Weinheim: Wiley-VCH Verlag, Weinheim, 2000.
12. Mundy, A. P. and Boley, N.: A Survey of Instrumentation used for the Determination of Haze in Beer, Journal of the Institute of Brewing, **105** (1999), no. 2, pp. 75-78.
13. Polke, R. and Rieger, R.: Partikelgrößenanalysen < 10 µm Meßmethoden und Schwierigkeiten, Chemie Ingenieur Technik, **50** (1978), no. 3, pp. 149-154.
14. Fu, R.; Wang, C.; Muñoz, O.; Videen, G.; Santarpia, J. L. and Pan, Y.-L.: Elastic back-scattering patterns via particle surface roughness and orientation from single trapped airborne aerosol particles, Journal of Quantitative Spectroscopy and Radiative Transfer, **187** (2017), pp. 224-231.
15. Dautzenberg, H. and Gröbe, V.: Die Lichtstreuung – eine geeignete Methode zur Untersuchung von Polymerfällungsprozessen; Acta Polymerica, **35** (1984), no. 7, pp. 523-526.
16. Kraemer, B.: Laboruntersuchungen zum Gefrierprozeß in polaren stratosphärischen Wolken, dissertation, FU - Berlin, 1998, pp. 14-16.
17. Ray, A. K.; Souyri, A.; Davis, E. J. and Allen, T. M.: Precision of light scattering techniques for measuring optical parameters of microspheres, Applied Optics, **30** (1991), no. 27, p. 3974.

Received 28 May 2018, accepted 17 June 2018